



## Research paper

# Strengthening of photovoltaic and supercapacitive properties of graphene oxide-polyaniline composite by dispersion of $\alpha$ -Al<sub>2</sub>O<sub>3</sub> nanoparticles

Kailash Nemade<sup>a,\*</sup>, Pradip Tekade<sup>b</sup>, Priyanka Dudhe<sup>b</sup><sup>a</sup> Department of Physics, Indira Mahavidyalaya, Kalamb 445 401, India<sup>b</sup> Department of Chemistry, Jankidevi Bajaj College of Science, Wardha 442 001, India

## ARTICLE INFO

## Article history:

Received 3 May 2018

In final form 8 July 2018

Available online 10 July 2018

## Keywords:

Graphene oxide

Polyaniline

Photovoltaic

Supercapacitive properties

## ABSTRACT

It is demonstrated that the dispersion of  $\alpha$ -Al<sub>2</sub>O<sub>3</sub> nanoparticles in graphene oxide (GO)-polyaniline (PANi) composite results in significant enhancement of photovoltaic and supercapacitive properties. In order to improve PV and SC properties of GO-PANi composite, 0.5 wt% of  $\alpha$ -Al<sub>2</sub>O<sub>3</sub> nanoparticles were added in composite. Both PV and SC properties of composites becomes strengthen by addition of 0.5 wt% of  $\alpha$ -Al<sub>2</sub>O<sub>3</sub> nanoparticles. The GO-PANi/ $\alpha$ -Al<sub>2</sub>O<sub>3</sub> composite shows power conversion efficiency ( $\eta$ ) 9.31%, which is significantly higher than pure  $\alpha$ -Al<sub>2</sub>O<sub>3</sub> nanoparticles and GO-PANi composite. The GO-PANi/ $\alpha$ -Al<sub>2</sub>O<sub>3</sub> composite achieve considerable specific capacitance of the order 715.5 Fg<sup>-1</sup> at scan rate of 2 mV s<sup>-1</sup>.

© 2018 Elsevier B.V. All rights reserved.

## 1. Introduction

The widespread use of inorganic photovoltaic cell is still limited because of complications in modification of band gap of inorganic materials and high processing costs [1]. Different approaches using organic or polymer materials such as conducting polymer, graphene and metal oxides have received considerable attention because of their low cost, light weight and flexibility [2]. Whereas supercapacitor is a new class of device, which comes under the category of energy storage devices, and fulfill the technological gap between conventional capacitor and battery. Supercapacitor has some outstanding features like power density, rapid store/release of energy, good charge/discharge life cycles, and Eco friendliness. For supercapacitor application, carbon nanomaterials such as carbon nanotubes and graphene are extensively used, due to their high specific surface area and good electrical conductivity [3].

The use of carbon nanostructures with the conducting polymer is also investigated as supercapacitive material extensively. Yu et al investigated the polyaniline/graphene composite as electrode material for supercapacitors. The electrochemical capacitance of composite has value 596.2 Fg<sup>-1</sup> and after 1500 cycles at a current density of 2 A g<sup>-1</sup>, only 16.3% drop in the initial capacitance is observed [4]. Wang et al synthesized PANi with different mor-

phologies and combined with graphene to use as electrode materials of supercapacitors. The result of the study shows that sheet-like Graphene/PANi composites can deliver specific capacitances of 532.3–304.9 Fg<sup>-1</sup> at scan rates of 2–50 mV/s [5]. Wu et al prepared the Polyaniline/graphene hydrogel composites for supercapacitor application with macroscopically phase-separated structure, which exhibits the high specific capacitance and excellent rate performance. This work concludes the PANi is mainly outside the graphene hydrogel matrix, can enhance the rate performance of the composites [6]. Cong et al prepared the graphene-PANi paper and employed for the supercapacitor application. The composite paper has considerable specific capacitance (763 Fg<sup>-1</sup>) and good cycling stability [7]. Moussa et al reviewed comprehensively the recent developments in polyaniline/graphene nanocomposites as supercapacitor electrodes. This work underlined the polyaniline/graphene nanocomposites have great potential in electrochemical energy storage applications, especially supercapacitors [8]. Theophile et al reported the successful preparation of Poly(vinyl alcohol)-graphene oxide and Poly(vinyl alcohol)-reduced graphene oxide composite for supercapacitor application. The results of the study indicates that Poly(vinyl alcohol)-reduced graphene oxide composite (190 Fg<sup>-1</sup>) deliver good supercapacitive properties than Poly(vinyl alcohol)-graphene oxide (13 Fg<sup>-1</sup>) composite [9]. Loeblein et al a novel material having oxidized-three-dimensional-graphene, with a band gap of 0.2 eV. This material found suitable for electrode application in dye-sensitized solar cells where electrode has stringent work-function requirements [10]. Li et al successfully

\* Corresponding author.

E-mail address: [knemade@gmail.com](mailto:knemade@gmail.com) (K. Nemade).

fabricated the PANi nanotubes-based supercapacitors having maximum areal capacitance of  $237.5 \text{ mF cm}^{-2}$  (scan rate =  $10 \text{ mVs}^{-1}$ ) with maximum energy density of  $24.31 \text{ mW h cm}^{-2}$  (power density =  $2.74 \text{ mW cm}^{-2}$ ). Under bending condition, supercapacitor shows excellent performance. After 2000 cycles, the capacitor maintains 95.2% of the initial capacitive value [11].

Feng et al prepared the graphene/polyaniline nanocomposites by using one-step hydrothermal method. The graphene/PANi nanowire composites exhibit the excellent electrochemical properties having specific capacitance  $724.6 \text{ F/g}$  higher than the graphene/PANi nanocomposite ( $602.5 \text{ F/g}$ ). This study demonstrated that morphology of materials also plays key role in optimization of electrochemical properties [12]. Zhou et al reported the effect of morphology on electrochemical properties using materials system nanoflake-like and nanobelt-like  $\alpha\text{-MoO}_3$ /graphene nanocomposites. The results of the investigation demonstrated that  $\alpha\text{-MoO}_3$  nanoflakes/graphene exhibited better supercapacitive (up to  $360 \text{ Fg}^{-1}$ ) performances than  $\alpha\text{-MoO}_3$  nanobelts/graphene [13].

In the light of above discussion, we planned to investigate the photovoltaic and primary electrochemical properties of  $\alpha\text{-Al}_2\text{O}_3$ /PANi-GO composite. In this work, we studied the PV cell properties such as fill factor and power conversion efficiency and supercapacitive properties such, cyclic voltammetry (CV) curve, areal capacitance and cycle stability performance of composite materials. The main accomplishment of present work is that we achieved considerable value of power conversion efficiency and specific capacitance for  $\alpha\text{-Al}_2\text{O}_3$ /PANi-GO composite.

## 2. Experimental

### 2.1. Materials preparation and characterization

In the present study, all AR-grade (SD Fine, India) chemicals were used for the preparation materials without further purification. The chemical oxidative polymerization was adopted for the

preparation of Polyaniline (PANi). The method of preparation of PANi is reported previously [14]. In this process, aniline monomer and ammonium persulphate were used with molar ratio 1:1 M for preparation of PANi in aqueous media. The addition of aniline monomer in oxidant under constant magnetic stirring results in dark greenish precipitated. As obtained precipitated was washed two times with distilled water and dried in oven for overnight. The fine powder of PANi was used for the preparation of composites. The graphene oxide (GO) used in this work was prepared by previously reported method [15]. The ex-situ approach was adopted for the preparation of composites. The GO loaded PANi composite was prepared by taking equal wt.% of both contents. Whereas,  $\alpha\text{-Al}_2\text{O}_3$  loaded-GO/PANi composite was prepared by taking 0.5 wt% concentration of  $\alpha\text{-Al}_2\text{O}_3$  nanoparticles. Both the composites prepared in organic media (Acetone).

The X-ray diffraction (XRD) patterns of as-prepared materials were recorded on Rigaku Miniflex-II using  $\text{CuK}\alpha$  radiation ( $\lambda = 1.54 \text{ \AA}$ ). The morphology of samples was investigated using scanning electron microscope (SEM) images obtained from JEOL JSM-7500F.

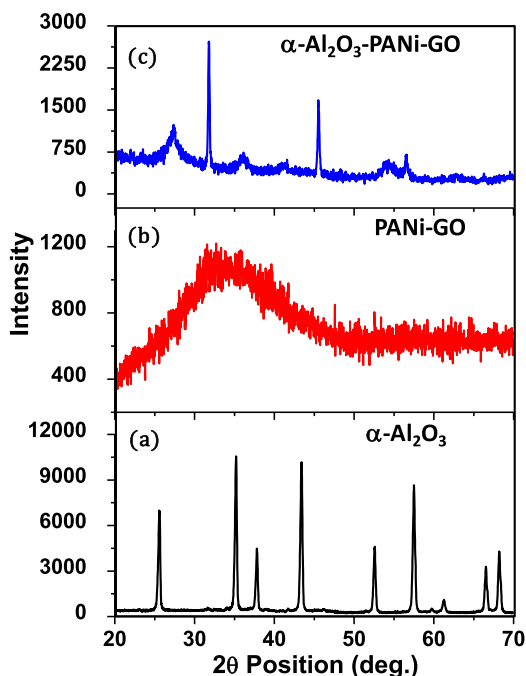


Fig. 1. XRD pattern of  $\alpha\text{-Al}_2\text{O}_3$  nanoparticle, PANi-GO and  $\alpha\text{-Al}_2\text{O}_3$ /PANi-GO composite.

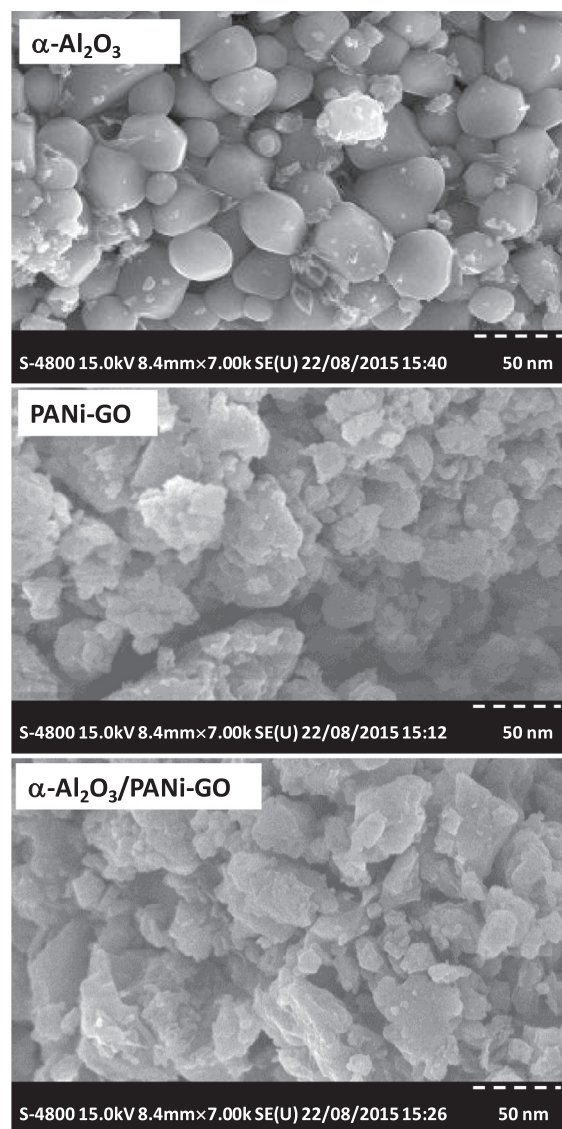


Fig. 2. FE-SEM images of  $\alpha\text{-Al}_2\text{O}_3$ , PANi-GO and  $\alpha\text{-Al}_2\text{O}_3$ /PANi-GO composite.

## 2.2. Supercapacitive study

Electrochemical measurements such as cyclic voltammetry (CV), areal capacitance and capacitance retention analysis were carried out using three-electrode cell systems (CHI 660 D, CH Instruments). As-prepared materials were used as the working electrode, platinum wire as counter electrode and Ag/AgCl as the reference electrode.

## 2.3. Photovoltaic (PV) study

PV cell required for testing was prepared by doctor blade technique. During the fabrication of PV cell, indium tin oxide (ITO) coated glass plate were used as transparent electrode and aluminum as metallic electrode. The photovoltaic properties of as-fabricated PV cell such as fill factor (FF) and power conversion efficiency ( $\% \eta$ ) confirmed by measuring short circuit current ( $I_{sc}$ ), open circuit voltage ( $V_{oc}$ ) and  $I_{max}$  and  $V_{max}$  from IV characteristics of PV cells.

## 3. Results and discussion

### 3.1. Characterization of materials

Fig. 1(a) shows the XRD pattern of  $\alpha$ -Al<sub>2</sub>O<sub>3</sub> nanoparticles, which is in good agreement with PDF Card No-01-081-1667. No other peaks for impurities were detected in pattern. The average crystallite size was computed by considering all prominent diffraction peaks using the Debye-Scherrer equation, which found to be 37.3 nm [16]. Fig. 1(b) depicts the XRD pattern of PANi-GO composite. The XRD pattern shows noisy behavior of diffraction peaks, which confirms the composite exhibited amorphous nature. In addition to this composite comprises broad

hump between  $2\theta$ -range 20–30°. Fig. 1(c) shows the XRD pattern of  $\alpha$ -Al<sub>2</sub>O<sub>3</sub> nanoparticles loaded PANi-GO composite. Pattern clearly indicates the presence of signature peaks of  $\alpha$ -Al<sub>2</sub>O<sub>3</sub> and GO. This indicates the nice incorporation of  $\alpha$ -Al<sub>2</sub>O<sub>3</sub> in PANi-GO composite.

Fig. 2 represents the SEM images of  $\alpha$ -Al<sub>2</sub>O<sub>3</sub>, PANi-GO and  $\alpha$ -Al<sub>2</sub>O<sub>3</sub>/PANi-GO composite. SEM image of  $\alpha$ -Al<sub>2</sub>O<sub>3</sub> shows the nanoparticles have irregular shape with well separated boundaries. The average crystallite size estimated using XRD analysis is in good agreement with SEM study. The SEM images of PANi-GO and  $\alpha$ -Al<sub>2</sub>O<sub>3</sub>/PANi-GO composite have almost identical morphology like petals or sheets structure.

### 3.2. PV study of materials

Fig. 3(a–c) shows IV characteristics of PV cell fabricated using the active PV material,  $\alpha$ -Al<sub>2</sub>O<sub>3</sub>, PANi-GO and  $\alpha$ -Al<sub>2</sub>O<sub>3</sub>/PANi-GO composite respectively and the PV parameters reflected by materials are listed in Table 1. From results, it is concluded that  $\alpha$ -Al<sub>2</sub>O<sub>3</sub> loaded PANi-GO composite achieve higher short circuit current ( $I_{sc}$ ) than pure  $\alpha$ -Al<sub>2</sub>O<sub>3</sub> and PANi-GO. This might be attributed to the good dispersion of  $\alpha$ -Al<sub>2</sub>O<sub>3</sub> in PANi-GO composite and good charge-transfer process within composite, which is evident in the higher value of  $I_{sc}$  [17]. There is a significant enhancement in

**Table 1**  
PV parameters of  $\alpha$ -Al<sub>2</sub>O<sub>3</sub>, PANi-GO and  $\alpha$ -Al<sub>2</sub>O<sub>3</sub>/PANi-GO composite.

Material	$I_{max}$ (mA)	$V_{max}$ (V)	$I_{sc}$ (mA)	$V_{oc}$ (V)	FF	$\% \eta$
$\alpha$ -Al <sub>2</sub> O <sub>3</sub>	23.8	0.2	23.8	0.7	0.285	1.61
PANi-GO	86	0.2	86	0.7	0.285	5.81
$\alpha$ -Al <sub>2</sub> O <sub>3</sub> /PANi-GO	137.7	0.2	137.7	0.8	0.25	9.31

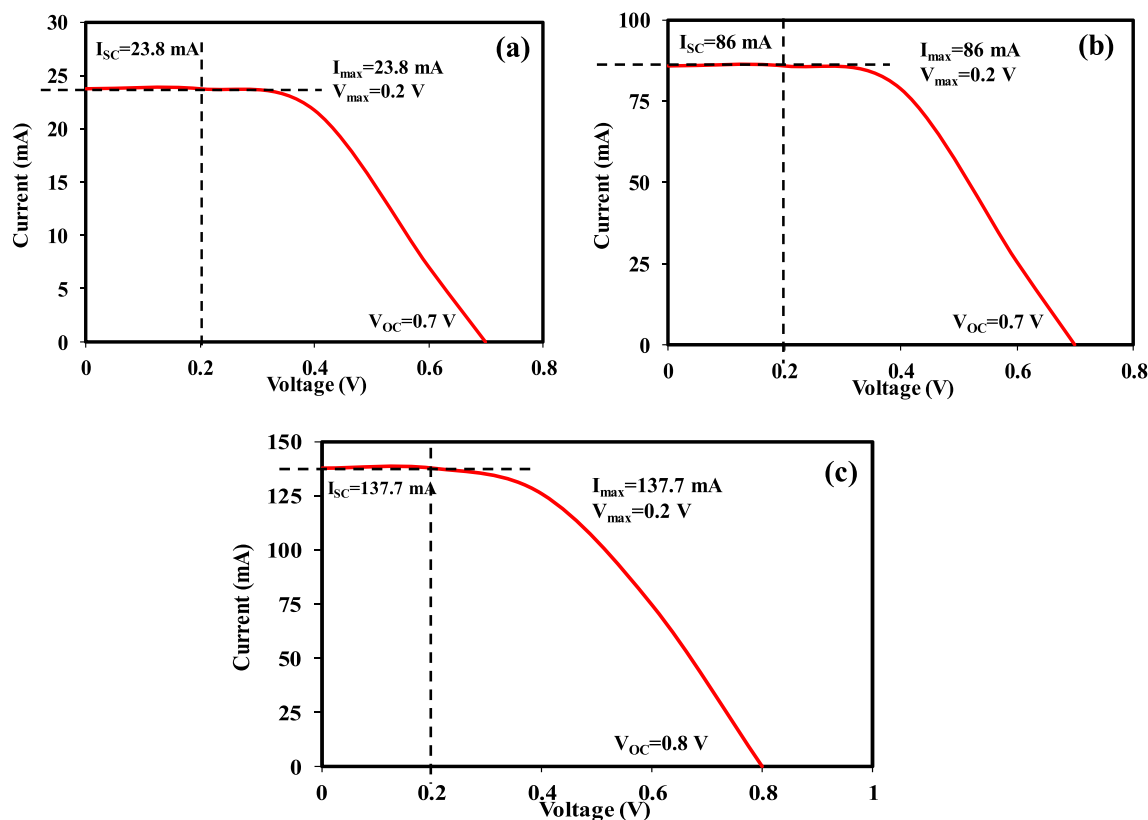


**Fig. 3.** PV response of (a)  $\alpha$ -Al<sub>2</sub>O<sub>3</sub>, (b) PANi-GO (c)  $\alpha$ -Al<sub>2</sub>O<sub>3</sub>/PANi-GO composite.

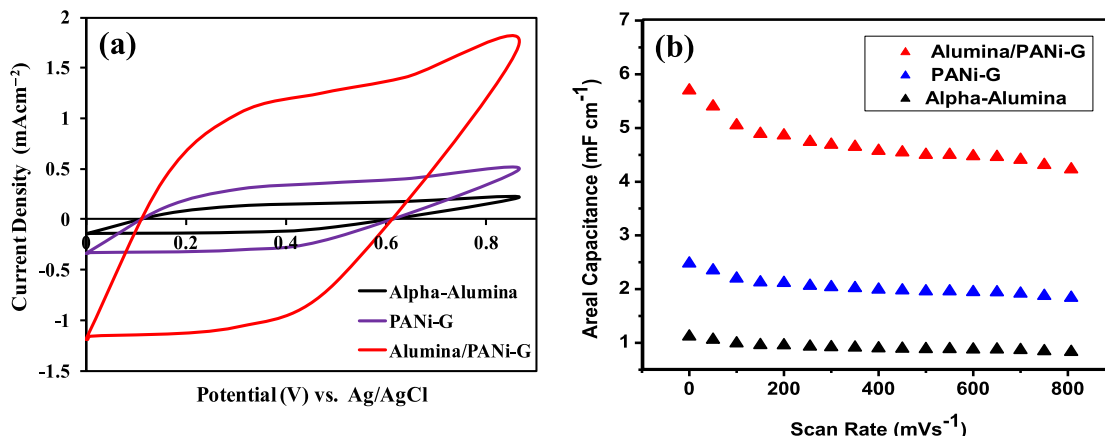


Fig. 4. (a) CV curves and (b) Areal capacitance as a function of scan rate of the  $\alpha$ -Al<sub>2</sub>O<sub>3</sub>, PANi-GO and  $\alpha$ -Al<sub>2</sub>O<sub>3</sub>/PANi-GO recorded at a scan rate of 2 mV s<sup>-1</sup>.

% $\eta$  resulted due to the addition of  $\alpha$ -Al<sub>2</sub>O<sub>3</sub> in PANi-GO composite. The highest value of % $\eta$  is 9.31% for  $\alpha$ -Al<sub>2</sub>O<sub>3</sub>/PANi-GO composite, whereas % $\eta$  is 5.81% for PANi-GO composite and 1.61% for  $\alpha$ -Al<sub>2</sub>O<sub>3</sub>.

### 3.3. Supercapacitive study of materials

Fig. 3a shows the cyclic voltammetric (CV) curves of  $\alpha$ -Al<sub>2</sub>O<sub>3</sub>, PANi-GO and  $\alpha$ -Al<sub>2</sub>O<sub>3</sub>/PANi-GO recorded at a scan rate of 2 mV s<sup>-1</sup>. The CV curves clearly shows the  $\alpha$ -Al<sub>2</sub>O<sub>3</sub>/PANi-GO composite have superior supercapacitive properties over pristine  $\alpha$ -Al<sub>2</sub>O<sub>3</sub>, PANi-GO composite. The superior supercapacitive properties of

$\alpha$ -Al<sub>2</sub>O<sub>3</sub>/PANi-GO composite can be attributed to oxidation/reduction of surface hydroxyl groups [18]. Specific capacitance has been estimated using the relation (Eq. (1)) [19],

$$C_s = \frac{I}{m \times v} (Fg^{-1}) \quad (1)$$

where  $I$  is the average current during anodic and cathodic scan (A),  $m$  is the mass of the electrode (g) and  $v$  is the scan rate (V). In our case, the highest value of specific capacitance was found to be 715.5 Fg<sup>-1</sup> at a scan rate of 2 mV s<sup>-1</sup> for  $\alpha$ -Al<sub>2</sub>O<sub>3</sub>/PANi-GO composite.

Fig. 3b shows the variation of calculated areal capacitance of the  $\alpha$ -Al<sub>2</sub>O<sub>3</sub>, PANi-GO and  $\alpha$ -Al<sub>2</sub>O<sub>3</sub>/PANi-GO composite as a function of scan rate. Here also plot clearly depicts that  $\alpha$ -Al<sub>2</sub>O<sub>3</sub>/PANi-GO composite has several fold higher capacitance over the pristine  $\alpha$ -Al<sub>2</sub>O<sub>3</sub>, PANi-GO composite. The significant enhancement in electrochemical performance was attributed to two main processes occurring in the composite. First is that composite possesses improved carrier density, which results in good electrical conductivity. Second is the increase of density of hydroxyl groups on  $\alpha$ -Al<sub>2</sub>O<sub>3</sub>/PANi-GO composite [20]. The absence of redox peak indicates that capacitance was mainly contributed by non-faradaic redox reactions.

As shown in Fig. 4, the capacitance drops in pristine  $\alpha$ -Al<sub>2</sub>O<sub>3</sub> and PANi-GO composite is significantly more than  $\alpha$ -Al<sub>2</sub>O<sub>3</sub>/PANi-GO composite. The  $\alpha$ -Al<sub>2</sub>O<sub>3</sub>/PANi-GO composite electrode exhibits an excellent long-term stability with 95.83% capacitance retention after 7000 cycles. The good capacitance ability of  $\alpha$ -Al<sub>2</sub>O<sub>3</sub>/PANi-GO composite is ascribed to enhanced electrical conductivity and highly stable surface redox reaction [21] (see Fig. 5).

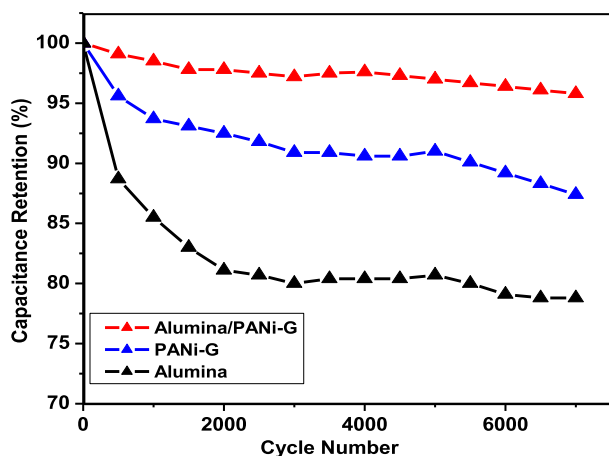


Fig. 5. Cycle performance of the alpha-Al<sub>2</sub>O<sub>3</sub>, PANi-GO and  $\alpha$ -Al<sub>2</sub>O<sub>3</sub>/PANi-GO composite measured at a scan rate of 2 mV s<sup>-1</sup> for 7000 cycles.

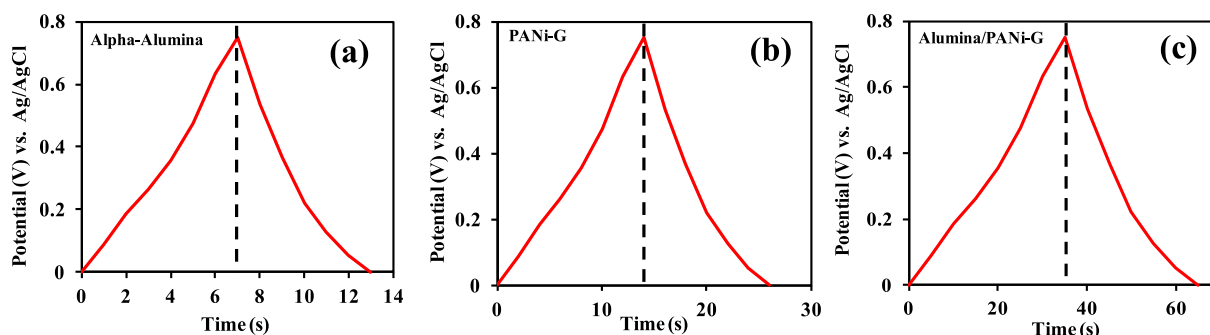


Fig. 6. Galvanostatic charge/discharge curves of the (a) alpha-Al<sub>2</sub>O<sub>3</sub>, (b) PANi-GO and (c) Al<sub>2</sub>O<sub>3</sub>/PANi-GO collected at a current density of 10  $\mu$ Acm<sup>-2</sup>.

Electrochemical study of  $\alpha$ - $\text{Al}_2\text{O}_3$ , PANi-GO and  $\text{Al}_2\text{O}_3$ /PANi-GO samples were extended by measuring charge/discharge measurements. Fig. 6(a–c) shows the galvanostatic charge/discharge (GCD) curves of  $\alpha$ - $\text{Al}_2\text{O}_3$ , PANi-GO and  $\text{Al}_2\text{O}_3$ /PANi-GO samples, respectively. The GCD curves of  $\text{Al}_2\text{O}_3$ /PANi-GO sample is nearly symmetric and significantly lengthy than  $\alpha$ - $\text{Al}_2\text{O}_3$  and PANi-GO. This indicates capacitive properties of  $\text{Al}_2\text{O}_3$ /PANi-GO sample superior than  $\alpha$ - $\text{Al}_2\text{O}_3$  and PANi-GO. Improved performance of  $\text{Al}_2\text{O}_3$ /PANi-GO attributed to synergetic state between  $\alpha$ - $\text{Al}_2\text{O}_3$  and PANi-GO.

#### 4. Conclusions

In summary, we have successfully demonstrated that the photovoltaic and supercapacitive performance of GO-PANi/ $\alpha$ - $\text{Al}_2\text{O}_3$  composite is superior over the  $\alpha$ - $\text{Al}_2\text{O}_3$  and PANi-GO composite. GO-PANi/ $\alpha$ - $\text{Al}_2\text{O}_3$  composite based PV cell shows significant power conversion efficiency of the order of 9.31%, which much higher than  $\alpha$ - $\text{Al}_2\text{O}_3$  and PANi-GO composite. The GO-PANi/ $\alpha$ - $\text{Al}_2\text{O}_3$  composite exhibits the considerable specific capacitance of the order  $715.5 \text{ Fg}^{-1}$ . The GO-PANi/ $\alpha$ - $\text{Al}_2\text{O}_3$  composite retain 95.83% capacitance after 7000 cycles, which shows the good cycling stability of composites. The GCD characteristics of  $\text{Al}_2\text{O}_3$ /PANi-GO sample improved due to synergetic effect between  $\alpha$ - $\text{Al}_2\text{O}_3$  and PANi-GO composite. At present work is underway for the optimization of the electrochemical performance GO-PANi/ $\alpha$ - $\text{Al}_2\text{O}_3$  composite.

#### Acknowledgment

The authors appreciate the help of Dr. S.K. Omanwar Head, Department of Physics, Sant Gadge Baba Amravati University, Amravati for providing necessary facilities for the work.

#### References

- [1] R.M. Swanson, *Progress in Photovolt.: Res. Appl. (Special Issue)* 14 (2006) 443–453.
- [2] N.S. Sariciftci, S.S. Sun, *Organic Photovoltaics: Mechanism, Materials, and Devices*, Taylor & Francis, New York, 2005.
- [3] M.F. El-Kady, V. Strong, S. Dubin, R.B. Kaner, Laser scribing of high-performance and flexible graphene-based electrochemical capacitors, *Science* 335 (2012) 1326–1330.
- [4] T. Yu, P. Zhu, Y. Xiong, H. Chen, S. Kang, H. Luo, S. Guan, Synthesis of microspherical polyaniline/graphene composites and their application in supercapacitors, *Electrochim. Acta* 222 (2016) 12–19.
- [5] R. Wang, M. Han, Q. Zhao, Z. Ren, X. Guo, C. Xu, N. Hu, L. Lu, Hydrothermal synthesis of nanostructured graphene/polyaniline composites as high-capacitance electrode materials for supercapacitors, *Scientific Reports* 7 (2017), Article number: 44562.
- [6] J. Wu, Q. Zhang, A. Zhou, Z. Huang, H. Bai, L. Li, Phase-separated polyaniline/graphene composite electrodes for high-rate electrochemical supercapacitors, *Adv. Mater.* 28 (2016) 10211–10216.
- [7] H. Cong, X. Ren, P. Wang, S. Yu, Flexible graphene–polyaniline composite paper for high-performance supercapacitor, *Energy Environ. Sci.* 6 (2013) 1185–1191.
- [8] M. Moussa, M. El-Kady, Z. Zhao, P. Majewski, J. Ma, Recent progress and performance evaluation for polyaniline/graphene nanocomposites as supercapacitor electrodes, *Nanotechnology* 27 (2016) 395201.
- [9] N. Theophile, H.K. Jeong, Electrochemical properties of poly(vinyl alcohol) and graphene oxide composite for supercapacitor applications, *Chem. Phys. Lett.* 669 (2017) 125–129.
- [10] M. Loeblein, A. Bruno, G.C. Loh, A. Bolkere, C. Saguy, L. Antila, S.H. Tsang, E.H.T. Teo, Investigation of electronic band structure and charge transfer mechanism of oxidized three-dimensional graphene as metal-free anodes material for dye sensitized solar cell application, *Chem. Phys. Lett.* 685 (2017) 442–450.
- [11] H. Li, J. Song, L. Wang, X. Feng, R. Liu, W. Zeng, Z. Huang, Y. Ma, L. Wang, Flexible all-solid-state supercapacitors based on polyaniline orderly nanotubes array, *Nanoscale* 9 (2017) 193–200.
- [12] X. Feng, N. Chen, J. Zhou, Y. Li, Z. Huang, L. Zhang, Y. Ma, L. Wang, X. Yan, Facile synthesis of shape-controlled graphene–polyaniline composites for high performance supercapacitor electrode materials, *New J. Chem.* 39 (2015) 2261–2268.
- [13] J. Zhou, J. Song, H. Li, X. Feng, Z. Huang, S. Chen, Y. Ma, L. Wang, X. Yan, The synthesis of shape-controlled  $\alpha$ - $\text{MoO}_3$ /graphene nanocomposites for high performance supercapacitors, *New J. Chem.* 39 (2015) 8780–8786.
- [14] K.R. Nemade, Chemically synthesized Sn doped polyaniline hydrochloride for carbon dioxide gas sensing, *Sensors Transducers* 135 (2011) 110–117.
- [15] K.R. Nemade, S.A. Waghuley, Chemiresistive gas sensing by few-layered graphene, *J. Electron. Mater.* 42 (2013) 2857–2866.
- [16] K.R. Nemade, S.A. Waghuley, Preparation of MnO<sub>2</sub> immobilized graphene nanocomposite by solid state diffusion route for LPG sensing, *J. Lumin.* 153 (2014) 194–197.
- [17] B. He, Q. Tang, M. Wang, H. Chen, S. Yuan, Robust polyaniline–graphene complex counter electrodes for efficient dye-sensitized solar cells, *ACS Appl. Mater. Interfaces* 6 (2014) 8230–8236.
- [18] D. Choi, G.E. Blomgren, P.N. Kumta, Fast and reversible surface redox reaction in nanocrystalline vanadium nitride supercapacitors, *Adv. Mater.* 18 (2006) 1178–1182.
- [19] B. Sethuraman, K.K. Purushothaman, G. Muralidharan, Synthesis of mesh-like Fe<sub>2</sub>O<sub>3</sub>/C nanocomposite via greener route for high performance supercapacitors, *RSC Adv.* 4 (2014) 4631–4636.
- [20] X. Lu, G. Wang, T. Zhai, M. Yu, J. Gan, Y. Tong, Y. Li, Hydrogenated TiO<sub>2</sub> nanotube arrays for supercapacitors, *Nano Lett.* 12 (2012) 1690–1696.
- [21] M. Kaempgen, C.K. Chan, J. Ma, Y. Cui, G. Gruner, Printable thin film supercapacitors using single-walled carbon nanotubes, *Nano Lett.* 9 (2009) 1872–1876.